Sensing Polymer Chain Dynamics through Ring Topology: A Neutron Spin Echo Study

Sebastian Gooßen,[1,*] Margarita Krutyeva,[1] Melissa Sharp,[2,3] Artem Feoktystov,[4] Jürgen Allgaier,[1]
Wim Pyckhout-Hintzen,[1] Andreas Wischnewski,[1] and Dieter Richter[1]

[1]*Jülich Centre for Neutron Science (JCNS-1) and Institute for Complex Systems (ICS-1),
Forschungszentrum Jülich GmbH, 52425 Jülich, Germany*
[2]*Institute Laue-Langevin (ILL), 38042 Grenoble Cedex 9, France*
[3]*European Spallation Source ESS AB, 221 00 Lund, Sweden*
[4]*Jülich Centre for Neutron Science (JCNS) at Heinz Maier-Leibnitz Zentrum (MLZ),
Forschungszentrum Jülich GmbH, Lichtenbergstraße 1, 85747 Garching, Germany*

Using neutron spin echo spectroscopy, we show that the segmental dynamics of polymer rings immersed in linear chains is completely controlled by the host. This transforms rings into ideal probes for studying the entanglement dynamics of the embedding matrix. As a consequence of the unique ring topology, in long chain matrices the entanglement spacing is directly revealed, unaffected by local reptation of the host molecules beyond this distance. In shorter entangled matrices, where in the time frame of the experiment secondary effects such as contour length fluctuations or constraint release could play a role, the ring motion reveals that the contour length fluctuation is weaker than assumed in state-of-the-art rheology and that the constraint release is negligible. We expect that rings, as topological probes, will also grant direct access to molecular aspects of polymer motion which have been inaccessible until now within chains adhering to more complex architectures.

Owing to their unique topology, macromolecular rings without chain ends are the subject of intense interdisciplinary research [1,2]. In biology, for instance, plasmids, cyclic polysaccharides [3], peptides [4], RNA [5], or DNA [6], are investigated, where nature exploits the ring topology to facilitate supercoiling or catenating [7]. Furthermore, in the fields of material science and engineering, blends of different polymer architectures including rings are employed aiming to produce polymer materials with emerging properties [8,9]. Recently, simulation science in particular led to new insights into ring dynamics on a coarse grained level [10,11]. In chemistry, novel procedures have enabled the production of appreciable amounts of pure, well-defined rings [12–16] that in turn permit detailed physical investigations of their structure and dynamics.

One of the important and fundamental goals of this broad approach is the understanding of entangled polymer dynamics far beyond the state-of-the-art standpoint. For cyclic polymers, reptation as well as the related relaxation through contour length fluctuations (CLFs) and constraint release (CR) are fully suppressed, requiring qualitatively different relaxation behavior in ring melts. The center of mass (c.m.) motion in such melts was found to be subdiffusive, characterized by a $t^{3/4}$ power law [17] which was understood in terms of the lattice animal theory [18] as well as in a recent approach of the diffusion of centrality [19]. Very recently the internal dynamics was also successfully addressed experimentally [17]: Rings relax via a combination of free internal loop-motion and loop

migration. As a result, the mean-square displacement for internal segment motion follows a weak $t^{0.3}$ power law, a finding also supported by simulation [20].

The unique ring topology also severely affects the ring structure and dynamics when blended with linear chains. Simulations showed that other than in the ring melts the ring conformation is close to Gaussian and no compaction is visible, at least in the range of ring concentrations below overlap [21]. On the other hand, rheological investigations display a very strong influence of small amounts of linear chains on the rheological response of a ring melt [22]. Threading linear chains through the rings crucially influences the long-range diffusion of rings [23,24], e.g., single-molecule spectroscopy revealed an extremely broad distribution of ring diffusion coefficients [25]. Recently, large-scale MD simulations on the diffusion and viscosity of ring–linear-chain blends were presented [11]. These simulations displayed a very significant increase in the viscosity and a strong decrease in diffusion at low ring concentration. Up to now no results on the internal dynamics of rings immersed in a linear melt have been presented.

In this Letter we show that in ring–linear-chain blends at low ring concentration the segmental ring dynamics is controlled by the host and differs qualitatively from that of the ring melts. The ring topology suppresses ring segmental motion beyond the entanglement constraints imposed by the host. In this way, the fundamental length scale of all tube theories is directly and uniquely accessed—the lateral tube size corresponds to the unrelaxed plateau

modulus. In moderately entangled matrices, where on the time scale of the experiment chain end effects play a role, the ring motion directly reveals that CLF contributions are weaker than assumed in state-of-the-art rheological theories and show that at short times CR effects are negligible. The ring polymer used in this investigation was polyethylene oxide (PEO) synthesized as described previously [17,26]. The characterization yielded $M_n = 20\,100$ g/mol (20k) using nuclear magnetic resonance (^{1}H NMR). For the deuterated linear polymers molecular weights corresponding to hydrogenous polymers with $M_n = 1790$ g/mol (2k), $M_n = 21\,300$ g/mol (20k), and $M_n = 82\,500$ g/mol (80k) were obtained by size exclusion chromatography (SEC) with PEO calibration. SEC revealed polydispersity indices $M_w/M_n \leq 1.05$ for all polymers. Blends of the ring polymer and the linear polymer were prepared in solution and freeze-dried from benzene. The volume fraction ϕ of the ring polymer in the blends was 0.1 for the neutron spin echo (NSE) spectroscopy studies and 0.01 for the small angle neutron scattering (SANS) experiment, respectively. In addition, for pulsed field gradient (PFG) NMR a blend of a linear polymer of identical molecular weight as the ring polymer with the deuterated 2k matrix was prepared ($\phi = 0.04$). The amount of hydrogenous polymer in the blends was chosen to be below the overlap concentration.

The SANS experiment was performed at KWS-1 at MLZ (Munich, Germany) [27]. NSE studies were carried out at the spectrometer IN15 at the ILL (Grenoble, France). For the PFG NMR experiments a Bruker Minispec (mq20) spectrometer was used. All measurements were performed at $T = 413$ K, well above the crystallization temperature. Figure 1 compares the SANS result of the 20k ring in the ring melt [17] with that of the 20k ring in a corresponding linear 20k melt under dilute conditions ($\phi = 0.01$). The solid red line presents the prediction for a Gaussian ring,

$$P(Q) = \frac{1}{N^2} \sum_{i,j} \exp\left[-\frac{1}{6}Q^2 l^2 |i-j|\left(1 - \frac{|i-j|}{N}\right)\right], \quad (1)$$

with Q the scattering vector, N the number of monomer segments, and l the statistical segment length per monomer (l was fitted to 5.9 Å). The dashed blue line describes the compact ring structure in the corresponding ring melt [17]. From Fig. 1 it is clear that in a linear matrix the ring assumes an unperturbed Gaussian conformation that is significantly more expanded than that of the corresponding ring melt. The radius of gyration $R_g = 36.5$ Å is 20% larger than the corresponding 30.5 Å in the pure ring melt.

Figure 2 presents the dynamic structure factor $S(Q,t)/S(Q)$ for the 20k ring in a short nonentangled melt of 2 kg/mol chains ($\phi = 0.1$). We stress the extraordinarily long time range of up to 600 ns that was covered in the NSE experiment. The lower insert presents PFG NMR data on the same system including also diffusion results for the corresponding 20k linear chain in the same matrix. The
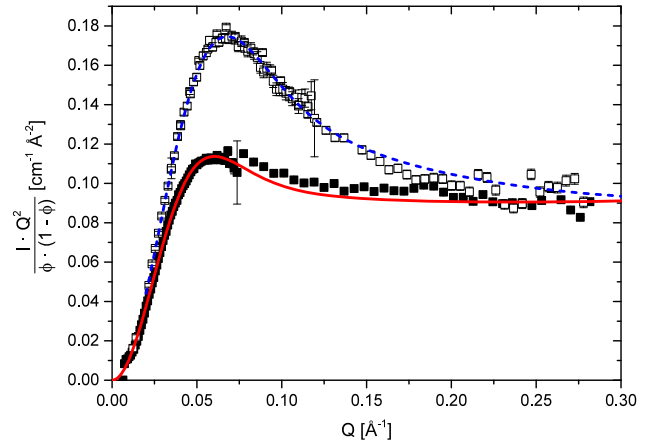

FIG. 1 (color online). SANS data for the 20k ring ($\phi = 0.01$) in a deuterated linear 20k matrix (full symbols) as compared to a pure ring polymer melt of identical molecular weight (empty symbols, data from [17]) in the Kratky representation. The lines represent fits to the data considering a Gaussian ring and a compact ring, respectively.

insert shows the self-correlation function $S_{\text{self}}^{\text{NMR}}(Q^2 t)$ as the function of $Q^2 t$, where Q relates to the field gradient and t to the distance between pulses [28,29]. The initial decay of the echo amplitude relates to the diffusion of the short chains measured independently on the corresponding short chain melt. The decay at larger $Q^2 t$ stems from the ring or the long linear chain, respectively. It is obvious that the ring and the linear chain display identical c.m. diffusion
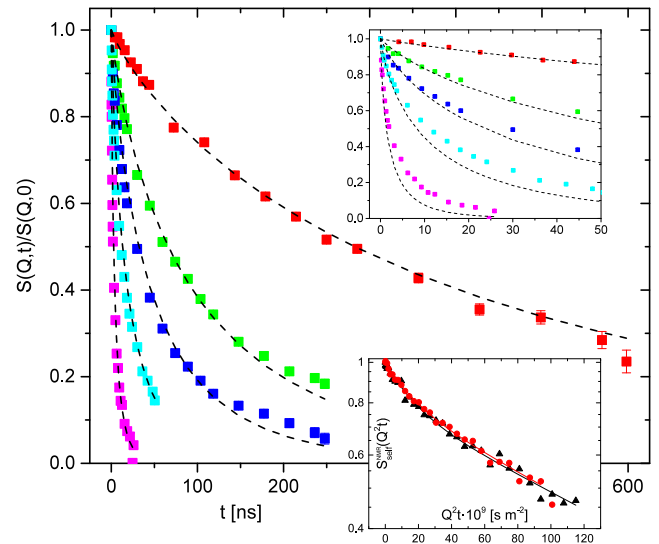

FIG. 2 (color online). NSE spectra for the 20k ring ($\phi = 0.1$) in a deuterated linear 2k matrix for Q values (from the top down) 0.05, 0.08, 0.1, 0.13, and 0.2 Å^{-1} at $T = 413$ K. Upper inset: NSE data at a shorter time scale. The dashed black lines represent fits to the data (for details see text). Lower inset: PFG NMR data of a 20k ring (red circles) and a linear 20k chain (black triangles) in a deuterated 2k matrix at $T = 413$ K.

behavior. Seemingly, the topology is unimportant and only the friction of the polymer segments with the surrounding matrix influences diffusion behavior. At 413 K we find $D_{\text{ring}} = 0.49 \ \text{Å}^2 \, \text{ns}^{-1}$ and $D_{\text{lin}} = 0.48 \ \text{Å}^2 \, \text{ns}^{-1}$. We note that the translational diffusion for the 20k ring in long chain matrices is outside the detection limit of the NMR spectrometer ($D_{\text{trans}} \leq 10^{-3} \ \text{Å}^2 \, \text{ns}^{-1}$).

Furthermore, the ring is expected to perform unrestricted Rouse motion in the short nonentangled matrix. The dynamic structure factor was calculated [30] to

$$
S(Q,t) = \frac{1}{N} \sum_{i,j} \exp \Bigg[-\frac{\langle r_{\text{c.m.}}^2(t) \rangle Q^2}{6} - \frac{1}{6} Q^2 l^2 |i-j|
$$
$$
\times \left(1 - \frac{|i-j|}{N} \right) - \frac{4Q^2 N l^2}{6\pi^2} \sum_{p_{\text{even}}}^{N} \frac{1}{p^2}
$$
$$
\times \cos \left(p\pi \frac{(i-j)}{N} \right) \left(1 - \exp \frac{-t p^2}{\tau_R} \right) \Bigg] \qquad (2)
$$

with the Rouse time $\tau_R = (\xi_0 N^2 l^2 / 3\pi^2 k_B T)$ where ξ_0 is the monomeric friction coefficient and the c.m. mean-square displacement $\langle r_{\text{c.m.}}^2(t) \rangle \propto t^\beta$. In the Rouse regime, for linear chain melts β is found on the order of 0.8 [31,32]. The dashed lines in Fig. 2 present a fit with Eq. (2) tying the c.m. diffusion to the NMR result and fitting the stretching exponent β as well as the friction ξ_0. While $\beta = 0.83$ is well within the range of what is normal for the diffusion of linear chains, the apparent friction coefficient ξ_0 from the overall fit is about 3 times larger than expected from the translational diffusion. However, this larger friction coefficient does not describe the initial short time internal relaxation that is significantly faster. It is well described by the diffusion-related lower friction (see upper insert in Fig. 2). Apparently, the short chain melt does not simply act as a heat bath but couples to the internal ring relaxation modes and slows them down for longer times. Similar results were found on binary linear polyethylene melts [33].

In the following, we deal with the dynamics of rings in long entangled matrices. Figure 3 displays the results for the ring in an 80k PEO matrix. Compared to Fig. 2 the dynamic structure factor is fully altered, displaying a fast initial decay in time, followed by time-independent plateaus that vary with the momentum transfer Q. As mentioned above, the ring translational diffusion is strongly separated in time from the ring fluctuations that are observed by NSE; the data only reflect the internal ring motions. In the insert, the dashed lines present the corresponding results for the dynamics from the pure ring melt [17] devoid of the translational diffusion contribution. The lines completely disagree with the observations in the linear matrix. Neither the initial nor longer term dynamics is described. Seemingly, the internal motions qualitatively change: there is no sign of the loop dynamics or of the loop migration prominent in the pure ring system. This contrasts
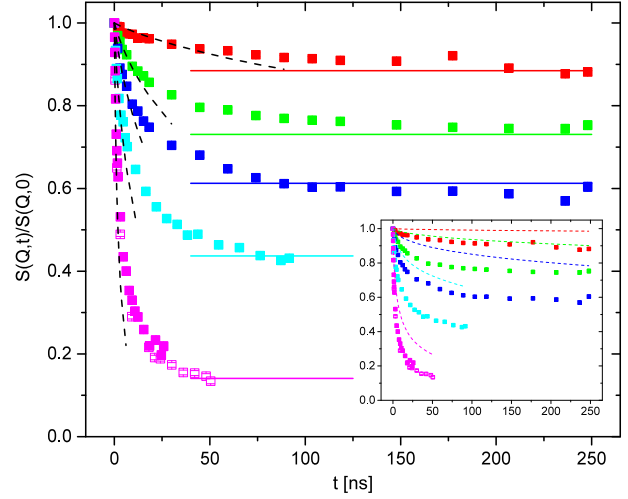

FIG. 3 (color online). NSE spectra for the 20k ring ($\phi = 0.1$) in a deuterated linear 80k matrix for Q values (from the top down) 0.05, 0.08, 0.1, 0.13, and 0.2 Å^{-1} at $T = 413$ K. Full and empty symbols refer to two different wavelength setups. Dashed black lines: initial Rouse decay. Solid lines: plateaus with $d_e = 42 \pm 1$ Å. Dashed colored lines: internal dynamics of pure 20k ring melt (data from Ref. [17]).

with assertions that ring motion in linear matrices may occur through loop formation extending through the walls of the tube [34]. The initially stronger decaying structure factor in the long chain blend compared to the ring melt points to much more freedom of motion than in the ring melts. The ring segments move as those of the linear chains and are subject to the same constraints. At the shortest times they enjoy free 3D Rouse motion inside the tube. This initial dynamics is very well described by the prediction of the Rouse dynamics for the ring [Eq. (2), dashed black lines]. For the initial relaxation all ring modes contribute in the Rouse fashion. For the calculations, the monomeric friction coefficient corresponding to the long chains was used.

After about 20–40 ns (≈ 1–$2\tau_e$), topological hindrance effects set in. $S(Q,t)$ crosses over towards time-independent but Q-dependent plateaus that, other than in entangled linear chains, do not decay any further. They manifest some solid constraints. Describing them with a Gaussian distribution of obstacles, such as the tube constraints $P_{\text{tube}}(Q) = \exp(-Q^2 d_e^2/36)$ we arrive at $d_e = 42 \pm 1$ Å. The predictions with $P_{\text{tube}}(Q)$ are indicated as solid parallel lines in Fig. 3 and describe the experimental findings very well. The confinement size $d_e = 42$ Å needs to be compared with the experimental results for the chain dynamics in linear melts where Niedzwiedz *et al.* found a tube diameter of $d = 52.5$ Å [35].

How do these two quantities relate to each other? The single chain pair correlation function $S(Q,t)$ for highly entangled linear chains contains the local reptation process, i.e., the relaxation of longitudinal Rouse modes along the

tube. The description of the dynamic structure factor in terms of this local reptation model then provides an effectively relaxed tube diameter d, relating to those constraints that remain after the relaxation by the longitudinal Rouse modes has finished. With respect to rheology, d relates to the corresponding relaxed plateau modulus. The ring segments, however, are not able to undergo longitudinal relaxation processes along the tube that is formed entirely by the confining linear chains. They remain confined by the lateral tube constraints and compare to the unrelaxed modulus. Thus, the ring directly probes the tube devoid of any further relaxation processes. The ratio of the relaxed and unrelaxed constraints $(d/d_e)^2 = 1.56 \pm 0.08 \approx 3/2$ expresses this fact. In the case of the linear chains, one third of the modes, i.e., the longitudinal modes, are not affected by the tube confinement [36]. Our investigation of ring dynamics in the highly entangled linear chain matrix directly reveals this relationship. Note, that as Likhtman and McLeish showed [37,38], the famous factor 4/5 between the relaxed and the unrelaxed modulus does not directly relate to the mean-square displacements measured in a scattering experiment.

Figure 4 presents the dynamic structure factor for the ring in a matrix of 20k linear analog chains. For comparison at $Q = 0.08$ Å^{-1} and $Q = 0.1$ Å^{-1} the results for the 80k blend are also included. Evidently, in the short but still significantly entangled 20k matrix (number of entanglements $Z \approx 10$) the ring is subject to further relaxation mechanisms. As we have seen, the ring probes the matrix dynamics. Therefore, these extra mechanisms must relate to the motions of the matrix that involve both CLFs and CR.
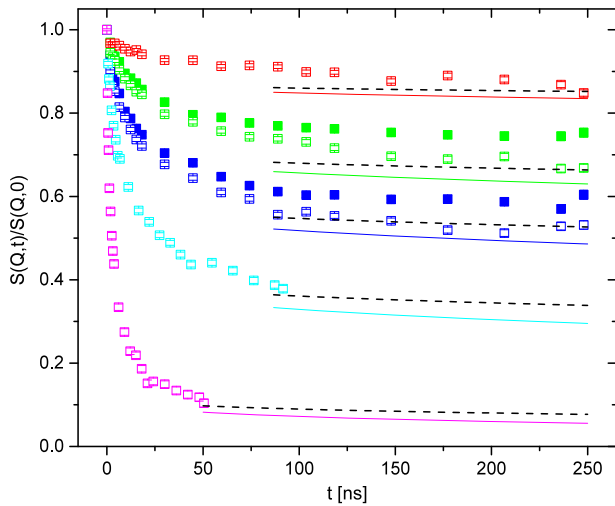
CLFs remove constraints for the chain segments via chain end fluctuations in a fixed tube, while constraint release originates from the removal of tube-forming chains by reptation. CLFs are considered to be dominant below the Rouse time ($\tau_R \approx 2$ μs). Recently, this was also demonstrated by a NSE experiment on a similar melt [39]. There, within the NSE window, the tube constraints not affected by CLFs (inner part of the chain) were found to be independent of time—CR was not active yet. Following Likhtman [40], the relative number of freed segments as a consequence of CLF is

$$\psi(t) = \frac{\alpha}{Z}\left(\frac{t}{\tau_e}\right)^{1/4} \qquad (3)$$

where $Z \approx 10$ is the number of entanglements and $\tau_e = \tau_R/Z^2 \approx 20$ ns is the entanglement time corresponding to d_e. Simulations yielded $\alpha = 1.5$ [37]. For the ring polymer that, as we have seen for the high M_w matrix, is confined by the unrelaxed tube, the freed linear chain segments will effectively dilate the tube similar to the widening of the tube by a solvent. As the concentration ϕ of confined linear chain segments will decrease with time the tube can be thought to widen as

$$d(t) = d_e\phi^{-0.5} = d_e/[1 - \psi(t)]^{0.5}. \qquad (4)$$

The dashed lines in Fig. 4 present the result of a fit of $S(Q, t > 100 \text{ ns})/S(Q)$ employing Eq. (4) in the tube form factor. The fit results in $\alpha = 1.1$, a value about 30% smaller than that used in the state-of-the-art Likhtman-McLeish (LM) rheological model. For comparison, Fig. 4 also displays the prediction for $\alpha = 1.5$ leading to a significant overprediction of the $S(Q,t)/S(Q)$ decay.

We note that, based on precise M_w dependent measurements of the plateau modulus, the Bailly group [41] also came to the conclusion that the LM model overestimates the CLF contribution by 30%. To rationalize this they proposed a time delay of τ_e for the onset of CLF, where τ_e is the time necessary for a lateral equilibration to take place across the tube. Our results confirm the overestimation of CLF on a molecular level. However, the suggestion of a time offset of τ_e is not supported. In Eq. (3) such an offset would result in only a 2% reduction of $\psi(t)$.

In the LM model, at early times ($t < \tau_R$) CR and CLF processes should have a similar effect. This is arrived at by squaring the CLF contribution. In this case the exponent in Eq. (4) would be 1 instead of 0.5. Hence, $\alpha = 0.55$ would result, a value clearly too low.

In conclusion, polymer rings have proved themselves to be a unique probe to investigate the matrix dynamics of long chains. We also anticipate that tube dilution effects prominent in branched architectures can, for example, be quantitatively addressed by a small number of immersed rings.

FIG. 4 (color online). NSE spectra for the 20k ring ($\phi = 0.1$) in a deuterated linear 20k matrix (empty symbols) for Q values (from the top down) 0.05, 0.08, 0.1, 0.13, and 0.2 Å^{-1} at $T = 413$ K. Full symbols: 20k ring in a linear 80k matrix. Dashed lines: fit to the data considering CLF with $\alpha = 1.1$. Thin solid lines: CLF contribution with $\alpha = 1.5$.

*s.goossen@fz-juelich.de

[1] T. McLeish, Science **297**, 2005 (2002).

[2] T. McLeish, Nat. Mater. **7**, 933 (2008).

[3] S. Kitamura, in *Cyclic Polymers*, edited by J. Semlyen (Springer, Netherlands, 2002), pp. 125–160.

[4] D. J. Craik, Science **311**, 1563 (2006).

[5] S. Memczak, M. Jens, A. Elefsinioti, F. Torti, J. Krueger, A. Rybak, L. Maier, S. D. Mackowiak, L. H. Gregersen, M. Munschauer, A. Loewer, U. Ziebold, M. Landthaler, C. Kocks, F. le Noble, and N. Rajewsky, Nature (London) **495**, 333 (2013).

[6] G. Witz, K. Rechendorff, J. Adamcik, and G. Dietler, Phys. Rev. Lett. **106**, 248301 (2011).

[7] L. Feng, R. Sha, N. C. Seeman, and P. M. Chaikin, Phys. Rev. Lett. **109**, 188301 (2012).

[8] R. G. Larson, Macromolecules **34**, 4556 (2001).

[9] K. Zhang, M. A. Lackey, Y. Wu, and G. N. Tew, J. Am. Chem. Soc. **133**, 6906 (2011).

[10] J. D. Halverson, W. B. Lee, G. S. Grest, A. Y. Grosberg, and K. Kremer, J. Chem. Phys. **134**, 204905 (2011).

[11] J. D. Halverson, G. S. Grest, A. Y. Grosberg, and K. Kremer, Phys. Rev. Lett. **108**, 038301 (2012).

[12] K. Endo, Adv. Polym. Sci. **217**, 121 (2008).

[13] B. A. Laurent and S. M. Grayson, Chem. Soc. Rev. **38**, 2202 (2009).

[14] H. R. Kricheldorf, J. Polym. Sci., Part A: Polym. Chem. **48**, 251 (2010).

[15] T. Yamamoto and Y. Tezuka, Polym. Chem. **2**, 1930 (2011).

[16] Z. Jia and M. J. Monteiro, J. Polym. Sci. Part A: Polym. Chem. **50**, 2085 (2012).

[17] S. Gooßen, A. R. Brás, M. Krutyeva, M. Sharp, P. Falus, A. Feoktystov, U. Gasser, W. Pyckhout-Hintzen, A. Wischnewski, and D. Richter, Phys. Rev. Lett. **113**, 168302 (2014).

[18] M. Rubinstein, Phys. Rev. Lett. **57**, 3023 (1986).

[19] S. T. Milner and J. D. Newhall, Phys. Rev. Lett. **105**, 208302 (2010).

[20] K. Hur, R. G. Winkler, and D. Y. Yoon, Macromolecules **39**, 3975 (2006).

[21] B. V. S. Iyer, A. K. Lele, and S. Shanbhag, Macromolecules **40**, 5995 (2007).

[22] M. Kapnistos, M. Lang, D. Vlassopoulos, W. Pyckhout-Hintzen, D. Richter, D. Cho, T. Chang, and M. Rubinstein, Nat. Mater. **7**, 997 (2008).

[23] P. J. Mills, J. W. Mayer, E. J. Kramer, G. Hadziioannou, P. Lutz, C. Strazielle, P. Rempp, and A. J. Kovacs, Macromolecules **20**, 513 (1987).

[24] D. G. Tsalikis and V. G. Mavrantzas, ACS Macro Lett. **3**, 763 (2014).

[25] S. Habuchi, N. Satoh, T. Yamamoto, Y. Tezuka, and M. Vacha, Angew. Chem., Int. Ed. **49**, 1418 (2010).

[26] A. R. Brás, S. Gooßen, M. Krutyeva, A. Radulescu, B. Farago, J. Allgaier, W. Pyckhout-Hintzen, A. Wischnewski, and D. Richter, Soft Matter **10**, 3649 (2014).

[27] A. V. Feoktystov, H. Frielinghaus, Z. Di, S. Jaksch, V. Pipich, M.-S. Appavou, E. Babcock, R. Hanslik, R. Engels, G. Kemmerling, H. Kleines, A. Ioffe, D. Richter, and T. Brückel, J. Appl. Crystallogr. **48**, 61 (2015).

[28] E. O. Stejskal and J. E. Tanner, J. Chem. Phys. **42**, 288 (1965).

[29] G. Fleischer and F. Fujara, in *Solid-State NMR I Methods*, edited by B. Blümich (Springer, Berlin, Heidelberg, 1994), pp. 159–207.

[30] G. Tsolou, N. Stratikis, C. Baig, P. S. Stephanou, and V. G. Mavrantzas, Macromolecules **43**, 10692 (2010).

[31] G. D. Smith, W. Paul, M. Monkenbusch, and D. Richter, J. Chem. Phys. **114**, 4285 (2001).

[32] W. Paul, Chem. Phys. **284**, 59 (2002).

[33] M. Zamponi, A. Wischnewski, M. Monkenbusch, L. Willner, D. Richter, A. E. Likhtman, G. Kali, and B. Farago, Phys. Rev. Lett. **96**, 238302 (2006).

[34] T. Cosgrove, M. J. Turner, P. C. Griffiths, J. Hollingshurst, M. J. Shenton, and J. A. Semlyen, Polymer **37**, 1535 (1996).

[35] K. Niedzwiedz, A. Wischnewski, W. Pyckhout-Hintzen, J. Allgaier, D. Richter, and A. Faraone, Macromolecules **41**, 4866 (2008).

[36] S. T. Milner and T. C. B. McLeish, Phys. Rev. Lett. **81**, 725 (1998).

[37] A. E. Likhtman and T. C. B. McLeish, Macromolecules **35**, 6332 (2002).

[38] T. C. B. McLeish, Adv. Phys. **51**, 1379 (2002).

[39] M. Zamponi, M. Monkenbusch, L. Willner, A. Wischnewski, B. Farago, and D. Richter, Europhys. Lett. **72**, 1039 (2005).

[40] A. E. Likhtman, Macromolecules **38**, 6128 (2005).

[41] C. Liu, J. He, R. Keunings, and C. Bailly, Macromolecules **39**, 3093 (2006).